Automatic State Recognition of Multi-type Protection Platens based on YOLOv5 and Parallel Multi-Decision Algorithm

Ying Zhang[1], Yihui Zhang[2], Hao Wu[3], Boxiong Fu[4], Ling He[5]*
State Grid Shijiazhuang Electric Power Supply Company, Shijiazhuang, China[1, 2, 3, 4]
College of Electrical Engineering, Sichuan University, Chengdu, China[5]

***Abstract*—A protection platen is a vital component in relay protection systems. The manual inspection of protection platen states is long-term repetitive work with low efficiency and imposes a heavy burden on workers. In this work, we propose a new system to automatically detect the states of multi-type protection platens in images. This system can classify two protection platen categories and further recognize the states of protection platens. For the classification of protection platen types, we propose a new algorithm that automatically detects two protection platen types based on HSV (Hue, Saturation, Value) color space weighting operators. The proposed operators quantify the color variation in the protection platen and reduce the influence of environmental factors. With respect to the state recognition of protection platens, the Type-I protection platen states are automatically classified by the YOLOv5 (You only look once version 5) network. Since the Type-II protection platen has three primary states and more complicated structures, we investigate a new parallel multi-decision algorithm to recognize the states of Type-II protection platens based on the newly proposed watershed-color space difference-shape feature (W-CD-SF) method and the YOLOv5 network. The W-CD-SF technique can segment the protection platens and extract their shape features automatically. This multi-decision mechanism improves the robustness and generalization of state recognition. Experiments were conducted on the collected protection platen images containing 8,969 protection platens. The recognition accuracies of protection platen states exceed 95%. This system can provide auxiliary detection and long-term monitoring of protection platen states.**

Keywords*—Protection platen; parallel multi-decision; YOLOv5 network; watershed-color space difference-shape feature

I. INTRODUCTION

Relay protection systems ensure the security and stability of power system operation. A protection platen is a vital component in relay protection systems [1,2]. Protection platens require manual inspection during the operation process, and such inspection is long-term repetitive work with low efficiency, which places a heavy burden on workers [3,4]. An automatic tool can help relieve the aforementioned burden on and improve inspection efficiency. With this objective, image processing techniques can be adapted to provide auxiliary detection and long-term monitoring of protection platens.

There are many types of protection platens in relay protection systems. The most commonly used types, defined as Type-I and -II protection platens are illustrated in Fig. 1. The Type-I protection platens are shown in Fig. 1(a) while the Type-II protection platens are figured in Fig. 1(b). Type-I protection platens have two categories of states, i.e., “on” and “off,” while Type-II protection platens have three categories of states, i.e., “on,” “off,” and “standby.”

In existing studies, most researchers have conducted experiments based on the images of Type-I or -II protection platens. The relevant details of previous works are the following.

1) Image processing methods for recognizing different protection platen states: Gao Jian et al. [5] eliminated the influence of shadows in images caused by illumination based on the improved Otsu threshold method and adopted the Graham algorithm to detect the states of Type-II protection platens. They achieved a detection accuracy of 96.5% for 200 shadow images. Yao Jingyan et al. [6] used the RANSAC method to restore the highlight area and evaluated the state of the Type-II protection platen by calculating the dip angle of the plate’s edges. They tested their method with 200 images and achieved an accuracy of 93%. Zhenhan et al. [7] proposed a method of automatic recognition of protection platen states based on improved sparse representation. First, they detected highlight areas in images by evaluating the maximum distances between two classes and eliminated the detected highlight areas by the improved sparse algorithm. Then, the protection platen states were recognized by their calculated minimum external rectangle. The detection accuracy of Type-II protection platens in 240 images reached 97.92%. Chen Yueqing et al. [8] proposed an improved image searching algorithm that used the background-difference and optical flow methods to extract foreground objects and recognized the Type-I protection platen switch states based on extracted edges. However, this study does not provide recognition results for specific samples. Li Tiecheng et al. [9] automatically recognized the Type-I protection platen and its corresponding text label based on an image processing technique. Combined with a model clustering and matching algorithm, the protection platens’ row number and column number in images are obtained. The recognition accuracy is obtained by comparing the calculated locations and the manually labeled locations. Fu

*Corresponding Author
This work is supported by the State Grid Hebei Electric Power Technology Project (SGTYHT/21-JS-223).

Wenlong et al. [10] recognized the Type-I protection platen states based on morphological processing. They applied their method to the images collected from different places, and most of the protection platen states could be detected. The specific detection results were not given in their research.

2) Deep-learning networks for recognizing different protection platen states: Yuan Tuolai et al. [11] used the RPN algorithm to generate a detection box and delimit the search range and then used the trained fast RCNN algorithm to detect the valuable features in this range. The accuracy of detecting the Type-I protection platen states exceeded 94%. Based on the YOLOv5 algorithm, Shi Baohua et al. [12] proposed the EYOLO algorithm, designed the local residual aggregation module, globalized the local residual characteristics, and embedded the spatial attention mechanism into the residual block to maximize the role of the local residual module. The recognition accuracy of the Type-I protection platen states reached 94.07%. Chen Xiang et al. [13] proposed an improved target detection algorithm based on a lightweight perception-v3 network. The protection platen switch states are recognized based on the migration learning strategy. The experiment was conducted on 48 Type-I protection platen images. Yang Qianwen et al. [14] proposed a bilinear fine-grained recognition method. They integrated an attention mechanism to realize end-to-end recognition of Type-II protection platen states.

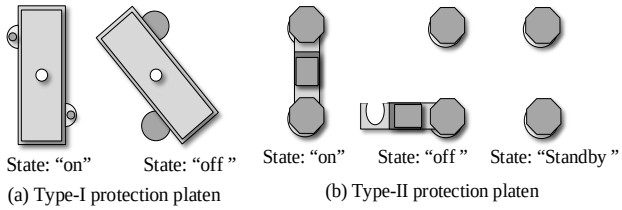

Fig. 1. Illustration of (a) Type-I and (b) Type-II Protection Platens.

The above studies illustrate that image processing methods and deep-learning networks can effectively detect protection platen states. However, these studies still have some limitations in practical applications. To overcome these limitations, we propose a new automatic state recognition system of multi-type protection platens based on the YOLOv5 and parallel multi-decision algorithms. The contributions of this work are as follows.

1) The existing studies can only recognize the states of one type of protection platen, namely a Type-I or -II protection platen. However, there are various types of protection platen in the actual operating environment. To solve this problem, we propose a new system that can classify multiple protection platen types and further recognize the states of protection platens automatically.

2) The proposed protection platen classification algorithm automatically detects two protection platen types based on HSV color space weighting operators. The proposed operators quantify the color variation in the protection platen region of interest (ROI) and reduce the influence of environmental factors through the operator weight settings of the H, S, and V color vectors.

3) A new parallel multi-decision algorithm is proposed to recognize the states of a Type-II protection platen in which parallel multi-decision is achieved by the newly proposed watershed-color space difference-shape feature (W-CD-SF) method and the YOLOv5 network. The W-CD-SF technique can segment the protection platens and extract their shape features automatically. The W-CD-SF with a support-vector-machine (SVM) classifier and YOLOv5 network classify the Type-II protection platen states in parallel, and then a fusion scheme is proposed to obtain the final detection results. This mechanism improves the robustness and generalization of the Type-II protection platen states recognition system.

II. METHODS

Automatic protection platen states recognition can help relieve the burden on workers, improve inspection efficiency, and provide long-term monitoring. In this section, we detail a new system that can classify two protection platen categories and further recognize the protection platen states automatically. First, two types of protection platens are classified by the newly designed HSV color space weighting operators. Second, two states of a Type-I protection platen are automatically classified using the YOLOv5 network. Compared with the Type-I protection platen, the Type-II protection platen has three basic states and more complicated structures. In this work, a parallel multi-decision algorithm is proposed based on the proposed W-CD-SF method and the YOLOv5 network. The structure of this system is depicted in Fig. 2.

A. Automatic Classification of Protection Platen Types based on HSV Color Space Weighting Operators

Automatic protection platen states classification is an important part of power protection system inspection. There are two commonly used protection platen types, and to detect protection platen states the types of protection platens are classified first. Based on the HSV color space, an automatic classification of the protection platen category algorithm is proposed in this work, and the method is shown in Fig. 3.

1) ROI exaction of the protection platens: As shown in Fig. 3, the ROI of each protection platen is segmented in the images using the morphological method. The Sobel operator is used to calculate the image edges. Filtering and threshold processing are applied to binarize the image edge. Based on the binary image edge, the smaller connected components are removed, and the bounding box of each protection platen connected component is extracted. Through the corresponding position of the bounding boxes, the ROI of each protection platen is segmented from the original images.

2) Classification of protection platen types based on HSV color space weighting operators: To classify the types of protection platens, HSV color space weighting operators are proposed in this work. The proposed HSV color space weighting operators quantify the overall color variation degree of the ROI. The color vectors H, S, and V in the HSV color space represent hue, saturation, and value, respectively.

Environmental factors, especially illumination, have the greatest influence on value variation, second-greatest on saturation variation, and least-greatest on hue variation. In this work, the color variation degree quantization operators are proposed for the above three vectors. To reduce the influence of environmental factors on color variation quantification, the operator weights are set as follows: The operator weight of hue is set to the maximum, followed by saturation, and the weight of value is set to the minimum. The structure of each operator is shown in Fig. 4. The color variation degree quantization operators for Hue, Saturation, Value vectors are illustrated in Fig. 4(a), (b) and (c), separately.

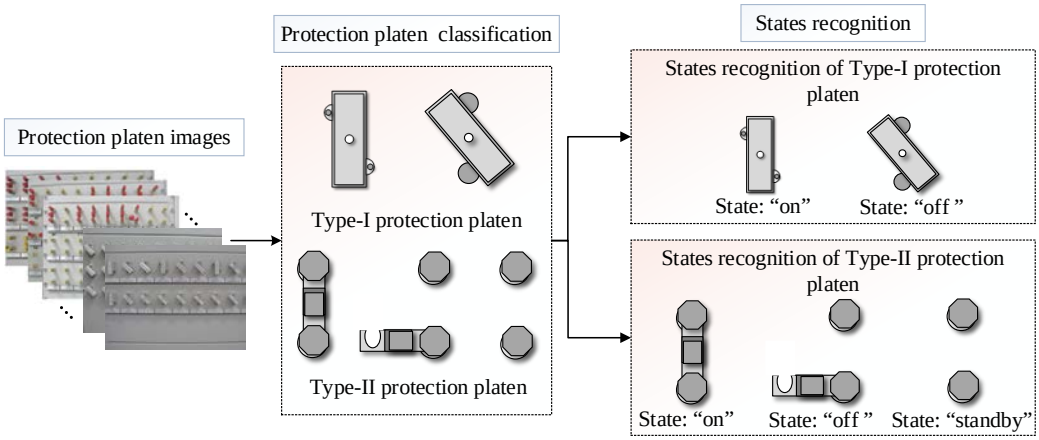

Fig. 2. Structure of Proposed Protection Platen States Recognition System.

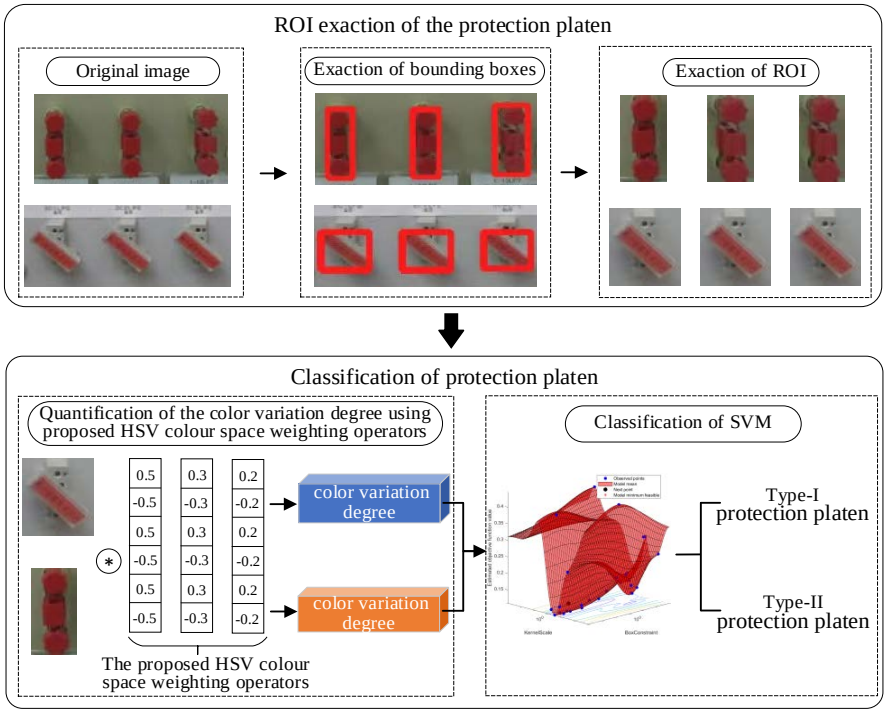

Fig. 3. Diagram of Automatic Protection Platen Category Classification Method.

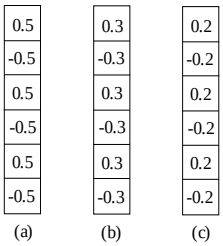

Fig. 4. Structure of Each Color Variation Degree Quantization Operator: Color Variation Degree Quantization Operator for (a) H, (b) S, and (c) V Vectors.

The length of each color variation degree quantization operator is consistent with the number of ROI rows. Each ROI column is traversed using the proposed operators, and the traversal sum of all columns is the calculated ROI color variation degree. The calculation formula of the ROI color variation degree (cv_{all}) is as follows:

$$cv_{all} = \sum_{j=1}^{n}\sum_{i=1}^{m} f_H(i,j)\cdot cell_H(i) + \sum_{j=1}^{n}\sum_{i=1}^{m} f_S(i,j)\cdot cell_S(i) + \sum_{j=1}^{n}\sum_{i=1}^{m} f_V(i,j)\cdot cell_V(i) \quad (1)$$

where $cell_H$, $cell_S$, and $cell_V$ denote the color variation degree quantization operator for the H, S, and V vectors, respectively. $f_H(i,j)$, $f_S(i,j)$, and $f_V(i,j)$ represent the corresponding pixel values of the point with coordinates (i,j) in the ROI. m and n represent the index of rows and columns of the ROI, respectively.

The mean value of cv_{all} of all ROIs in the image is the calculated color variation. Based on the quantified color variation, the protective panel images are divided into two categories combined with the SVM classifier.

B. *Automatic Detection of Type-I Protection Platen States based on YOLOv5*

In this work, the deep-learning network YOLOv5 is used to detect the states of Type-I protection platens, which have two categories of states: “on” and “off.”

In practical applications, multiple protection platens are densely distributed on the protective panel. The target detection of the protection platens belongs to small target detection because each protective panel experimental image has many small protection platens. The YOLOv5 network uses mosaic data enhancement [15], adaptive anchor box calculation [16], and adaptive image scaling at the input layer to improve the detection ability of small targets [17]. The small target detection ability of YOLOv5 is suitable for automatic protection platen detection in this work. In addition, the lightweight structure of YOLOv5 ensures the real-time detection requirements of protection platens in practical applications.

Regarding the overall framework of YOLOv5 shown in Fig. 5, the YOLOv5 network inherits the YOLOv4 structure, including the input layer, backbone network, neck, and prediction layer. It rescales the Type-I protection platen images to 608×608 size at the input layer. The rescaled input is divided into grids, and in each grid, the coordinates of the target boxes and their confidences are predicted. The confidence of the target box can be expressed as.

$$p = \Pr(Object) * IoU_{pred}^{truth} \quad (2)$$

Each target box carries the information of (x, y, w, h, p), where (x, y) is the relative coordinate of the normalized center point of target box, and (w, h) represents the width and height, respectively. The network outputs the corresponding prediction boxes according to the conditional probability values of the target boxes.

The input goes through the four kinds of modules of Focus, CBL, SSP, and CSPX_1 in the backbone network [18,19]. In the Focus module, the input is sliced, and then the sliced results are concatenated. The output of the Focus module is

$$Out_{Focus} = Concat(Slice(I_1, \cdots, I_n)) \quad (3)$$

where *Slice* represents reshape operation, the input image (A, B, C) is reshaped into $(A/n, B/n, C\times n\times n)$.

The output of the CBL module is

$$Out_{CBL} = \mathrm{Re}\,LU(BN(Conv(Input_{CBL}))) \quad (4)$$

where *Conv* represents the convolution, *BN* is the batch normalization, and $\mathrm{Re}\,LU$ is the activation function Leakly-ReLU.

In the CSPX_1 module, the input of the CSPX_1 module is shortcut connected:

$$Out_{CSPX\_1} = CBL(CBL(Input_{CSPX\_1})) + Input_{CSPX\_1} \quad (5)$$

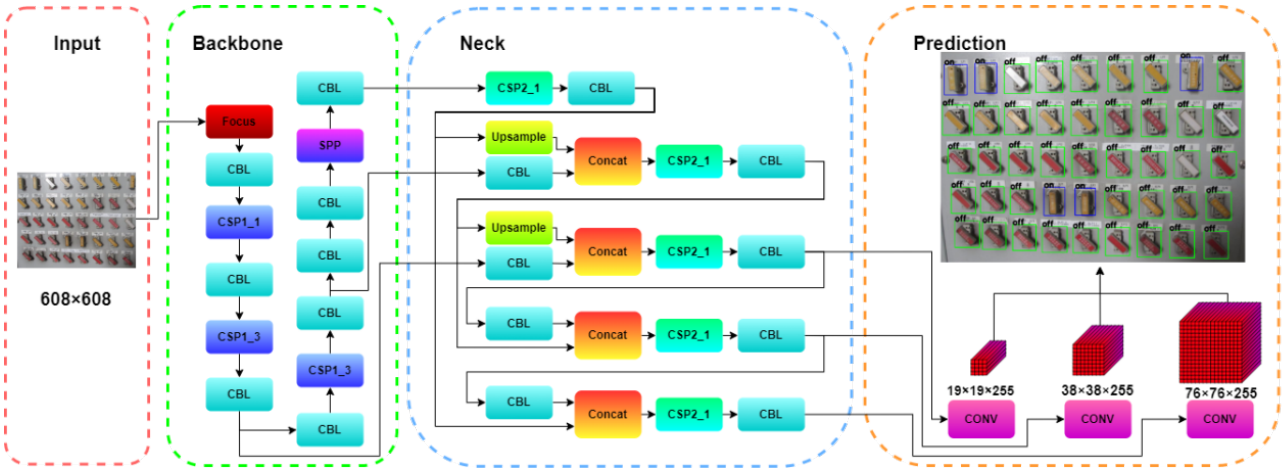

Fig. 5. Architecture of YOLOv5 for Automatic Recognition of Type-I Protection Platen States.

There are two operations in the SSP module, i.e., max-pooling and concatenation. The outputs of the SSP module are obtained as follows:

$$Out_{\mathrm{SSP}} = Concat(Maxpool(Input_{\mathrm{SSP}_1}, \cdots, Input_{\mathrm{SSP}_n})) \tag{6}$$

Through the backbone network, the feature maps of 20×20, 40×40, and 80×80 are obtained. The three sets of feature maps are combined by Neck (the structure combining FPN and PAN) for feature fusion detection. Neck outputs three feature map tensors, and the tensors are combined and passed to the prediction layer [20,21]. The prediction layer uses generalized intersection over union (GIoU) loss as the loss function and filters the target box through non-maximum suppression to obtain the final detection result. The GIoU loss is calculated as [22].

$$GIOU_{Loss} = 1 - IoU_B^A + \frac{\lfloor C(A \cup B) \rfloor}{|C|} \tag{7}$$

where A and B represent ground truth and predictions, respectively. C is the minimum closed area of A and B. Two states of Type-I protection platens are detected using the YOLOv5 network.

C. Parallel Multi-decision Algorithm for Type-II Protection Platen States Detection

The geometry and shooting background of Type-II protection platens are more complicated than those of Type-I protection platens. To achieve an accurate measurement, a parallel multi-decision algorithm is proposed based on the proposed W-CD-SF method and YOLOv5. First, the protection platens images are pre-processed to eliminate the highlight areas. Second, each protection platen is segmented based on the watershed method and color space difference information. The shape features are extracted from the segmented protection platens. Then, the states of the Type-II protection platens are automatically recognized using the proposed parallel multi-decision algorithm. The general overview of the proposed parallel multi-decision algorithm for type-II protection platen states detection is illustrated in Fig. 6.

1) Pre-processing: In this task, the quality of collected images is affected by the lighting, shooting distance, shooting angle, and other environmental factors. The highlights have a considerable influence on the protection platen segmentation. We adopt a method to detect and repair the highlight area. The details of this method are listed below.

a) Highlight area detection based on the proposed adaptive kurtosis threshold method: The detection and restoration of highlight areas are important in protection platen state detection. We propose an adaptive kurtosis threshold method to obtain a binarized mask image of the highlight areas automatically. The diagram of the proposed adaptive kurtosis threshold method is shown in Fig. 7.

Since the grey values of highlight areas differ greatly in adjacent regions of the protective panel images, the probability density curve of a grey image is adopted to evaluate the distribution of grey pixels. Generally, the highlight area is located at the back of the probability density curve due to its larger grey values. The probability density curve contains multiple peaks. The grey value corresponding to the rightmost peak is set as the adaptive threshold T_h. Based on the adaptive threshold; the binarized mask image of the highlight areas is calculated.

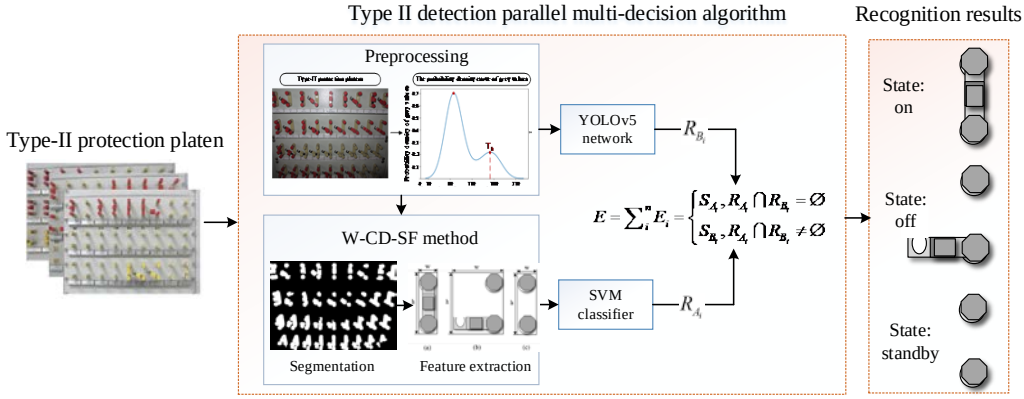

Fig. 6. General Overview of the Proposed Parallel Multi-decision Algorithm for Type-II Protection Platen States Detection.

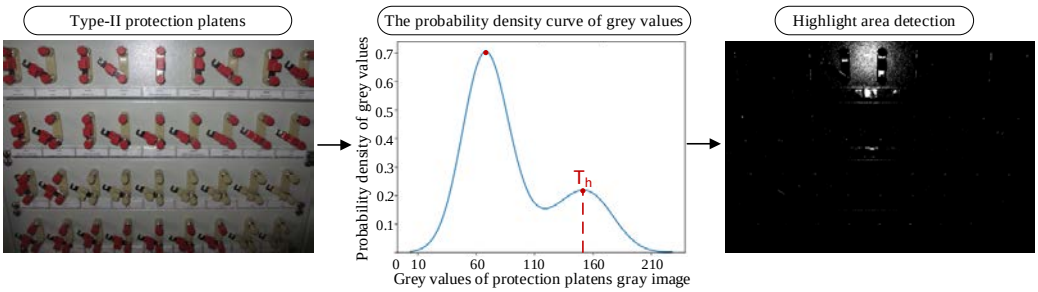

Fig. 7. Diagram of the Proposed Adaptive Kurtosis Threshold Method.

b) Highlight area restoration by using the fast march algorithm: The fast marching algorithm [23] is adopted to restore the detected highlight areas. The algorithm repairs the highlight areas from the boundaries of the non-zero regions in the mask image and updates the changes in the original image dynamically [24].

The fast marching algorithm fills the highlight area with pixels in its neighborhood [25]. To ensure natural filling, the weight function is adopted to distinguish the importance of different pixels in the neighborhood. The calculation formula of pixels to be filled is

$$I(p)=\frac{\sum_{q\in B_\varepsilon(p)}\omega(p,q)[I(q)+\nabla I(q)(p-q)]}{\sum_{q\in B_\varepsilon(p)}\omega(p,q)} \tag{8}$$

where $B_\varepsilon(p)$ denotes the neighborhood of the current pixel to be filled. $\omega(p,q)$ is the corresponding weight of neighborhood pixels, which is calculated as

$$\omega(p,q)=dir(p,q)\cdot dst(p,q)\cdot lev(p,q) \tag{9}$$

where $dir(p,q)$, $dst(p,q)$, and $lev(p,q)$ represent direction factor, geometric distance factor, and level set distance factor, respectively. The set of the above three factors ensures that the pixels closest to the normal, those closest to the pixel to be filled, and those closest to the contour of the highlight area to be repaired have the highest importance.

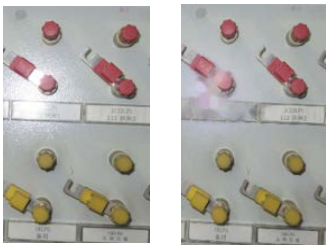

(a) (b)

Fig. 8. Illustration of Highlight Area Restoration in Protective Panel Images. (a) Original Images with Highlight Areas. (b) Restored Images.

When all the nonzero regions in the mask image are repaired, the highlight areas in the original image are also restored. An example of the highlight area restoration is shown in Fig. 8.

It is observed in Fig. 8 that the differences between the highlight area and its surrounding area are reduced.

2) Segmentation and feature extraction using the proposed W-CD-SF method: There are many protection platens in a protective panel image. To segment these protection platens, we propose a W-CD-SF method. The details of this method are introduced below.

a) Preliminary segmentation based on a watershed algorithm: The watershed algorithm is adopted to obtain the preliminary segmentation results of the protection platen. This algorithm is a transformation defined on a grayscale image. This transformation treats the image as a topographic map, with the brightness of each point representing its height, and finds the lines that run along the tops of ridges [26-29]. In this segmentation, we adopt this algorithm to obtain a continuous and close edge of each protection platen. Based on the close edge, each protection platen region can be extracted.

b) Irrelevant area elimination based on color space difference: In the second stage, we propose a new method to eliminate the irrelevant areas from segmented regions based on color difference. The irrelevant areas are mostly caused by uneven illumination and noise interference. There are color differences between the ROI and the irrelevant areas. In this method, the RGB color space is adopted to quantify the color differences. Fig. 9 shows the diagram of the proposed irrelevant area elimination method.

i) *Classification of sub-regions based on color distribution features:* Each image is divided into several 4 × 4 sub-regions. For each sub-region, the pixel value variances in the R, G, and B channels are calculated separately. The sum of the calculated pixel value variances in the three channels reflects the color distribution difference of the sub-region. Owing to the color difference between irrelevant areas and the ROI, the overall color distribution difference in the sub-region in which interference exists is greater than that in which interference does not exist. Based on the quantified color distribution difference, the sub-regions with irrelevant points are distinguished.

ii) *Interference points removal:* The pixels are arranged by their corresponding pixel value, and the first-order difference of the sorted pixel sequence difference is calculated to qualify the pixel value difference. In this work, the pixels with corresponding differences greater than the difference mean value are considered as interference points and removed.

c) Shape features extraction: To detect the states of Type-II protection platen, we extract the shape features of these segmented protection platens. These features are calculated based on the circumscribed rectangle of each protection platen's connected domain. The length h and width w of the circumscribed rectangle are obtained and illustrated in Fig. 10. Fig. 10(a), (b) and (c) correspond to the circumscribed rectangle for the state "on", "off" and "standby", respectively.

The bounding boxes of the Type-II protection platen obtained using the W-CD-SF method can be classified into two parts: protection platen region and noise. To eliminate the influence of noise and recognize the states of the Type-II protection platen more accurately, we propose the three following features with which to evaluate the shape of each bounding box:

$$HWR=\frac{h}{w} \tag{10}$$

$$CRA=h\times w \tag{11}$$

$$CRA_{mean}=\frac{\sum_i^n h_i \square w_i}{n} \tag{12}$$

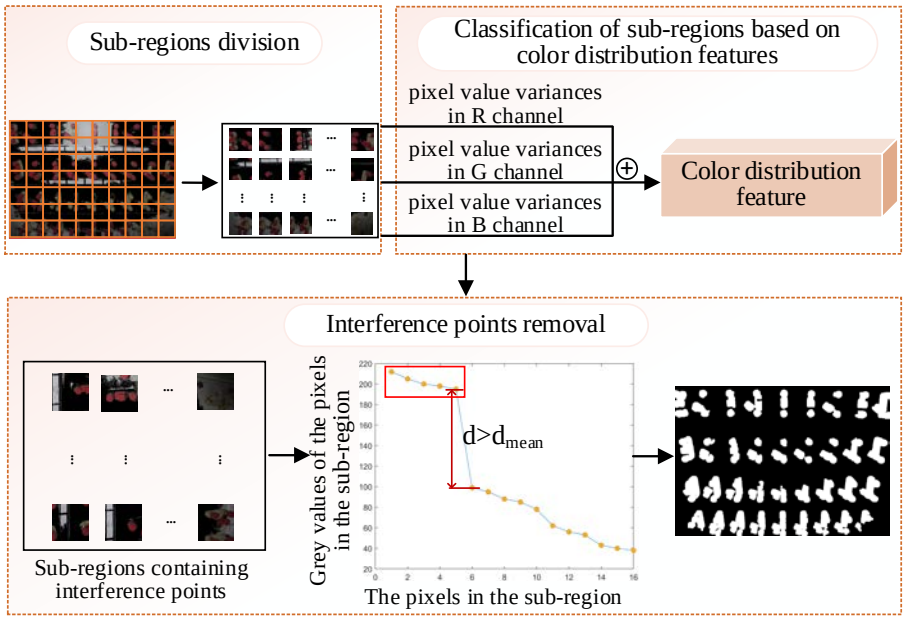

Fig. 9. Diagram of Proposed Irrelevant Area Elimination Method.

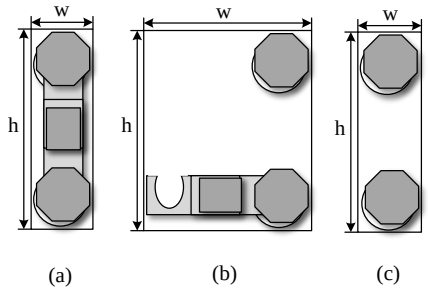

Fig. 10. Parameters Calculated from Each Connected Domain Circumscribed Rectangle: (a) State "on," (b) State "off," and (c) State "Standby."

where HWR is the ratio of h to w, CRA is the area of the circumscribed rectangle, and CRA_{mean} is the average area of a circumscribed rectangle of all detected objects. Finally, the Type-II protection platen states can be recognized using the segmentation masks and shape features combined with the SVM classifier.

3) Parallel multi-decision scheme based on W-CD-SF method and YOLOv5 network: The recognition result of Type-II protection platen using the W-CD-SF method is represented as A_i, which consists of the state category S_{A_i} (including states "on," "off," or "standby") and the bounding box region R_{A_i}. In addition, the state recognition result of the Type-II protection platen using YOLOv5 is represented as B_i, which is also composed of the state category S_{B_i} (including states "on", "off," or "standby") and the bounding box region R_{B_i}. The final state recognition result is the fusion of A_i and B_i.

Specifically, given the results of the W-CD-SF and YOLOv5 method, we can obtain the final states recognition result using the following rule:

$$E_i = \begin{cases} S_{A_i}, R_{A_i} \cap R_{B_i} = \varnothing \\ S_{B_i}, R_{A_i} \cap R_{B_i} \neq \varnothing \end{cases} \quad (13)$$

In this rule, if there is overlap between R_{A_i} and R_{B_i}, the final result is dependent on S_{B_i}, otherwise S_{A_i}.

III. Experimental Results and Analysis

The protection platen is an essential part of a relay protection inspection system. In this work, we propose a method to automatically detect the states of a protection platen. This method is composed of three parts: automatic protection platen type classification based on HSV color space weighting operators, Type-I protection platen state recognition based on YOLOv5, and Type-II protection platen state recognition based on the proposed parallel multi-decision mechanism. To evaluate the effectiveness of the proposed method, we conducted experiments on a protection platen image dataset. In this section, the dataset details, experimental settings, experimental results of automatic protection platen state recognition, along with the details of comparative experiments, are introduced and analyzed.

A. Dataset

The experimental data used in this work were collected by the State Grid Hebei Electric Power Company. There are two protection platens usually used in practical applications, i.e., Type-I and Type-II protection platens. In this work, the protective panel images containing these two types of protection platens are shot in various environments and include 3,625 Type-I protection platens and 5,344 Type-II protection platens.

B. Experimental Settings

This work achieves the automatic recognition of protection platen states. To evaluate the performance of the proposed

method, the 10-fold cross-validation method is applied. The performance of the system is evaluated in terms of accuracy, false positive rate (FPR), and false negative rate (FNR). Accuracy is the proportion of correctly predicted samples to total samples. FPR is the proportion of negative samples predicted to be positive to total negative samples, which reflects the probability of negative samples being misclassified. FNR is the proportion of positive samples predicted to be negative to total positive samples, which reflects the probability of missing detection of positive samples. The calculation formulas of accuracy, FPR, and FNR are respectively, where TP denotes the number of actually positive samples predicted to be positive samples, TN represents the number of actually negative samples predicted to be negative samples, FP is the number of actually negative samples predicted to be positive samples, and FN is the number of actually positive samples predicted to be negative samples.

$$\text{Accuracy}=\frac{TP+TN}{TP+FP+TN+FN} \tag{14}$$

$$\text{FPR}=\frac{FP}{FP+TN} \tag{15}$$

$$\text{FNR}=\frac{FN}{FN+TP} \tag{16}$$

The experiments were implemented based on the PyTorch framework. The YOLOv5 network was trained using batch size 8 for 300 epochs. The initial learning rate was set to 0.01, and the warmup technique was used for training YOLOv5. The learning rate warmup was set to 0.1. Adam was used as the optimization algorithm with a momentum of 0.8.

C. Experimental Results of Protection Platen States Recognition

The automatic recognition of protection platen states is a challenging task. The Type-I and -II protection platens have varied shapes. For one specific type, there are different colors of protection platens, and some protection platens and their protective panels are similar in color. Moreover, the shooting angle and distance are not the same, and the image quality is affected by lighting and shooting conditions, resulting in difficulties in recognizing the states of protection platens.

In this work, we propose utilizing the YOLOv5 network to recognize the Type-I protection platen state. Different from the Type-I protection platen, the shape of the Type-II protection platen is more complicated. To improve the recognition accuracy, in this work we propose a parallel multi-decision method combining the advantages of the proposed W-CD-SF method and YOLOv5 network.

The state classification results of Type-I and -II protection platens are listed in Tables I and II, respectively.

Table I shows that for the automatic state recognition task of Type-I protection platens the recognition accuracy, FPR, and FNR for the state "on" are 98.77%, 0%, and 1.23%, respectively. The recognition accuracy, FPR, and FNR for state "off" are 99.15%, 0%, and 0.85%, respectively. It can be seen from the results that the protection platen recognition accuracy of Type-I protection platens is over 98%, meeting the needs of practical applications.

TABLE I. TWO STATES RECOGNITION RESULTS OF TYPE-I PROTECTION PLATENS USING YOLOV5

State of protection platen	Number of protection platens	Accuracy	FPR	FNR
on	897	98.77%	0%	1.23%
off	2,728	99.15%	0%	0.85%

TABLE II. THREE STATES RECOGNITION RESULTS OF TYPE-II PROTECTION PLATENS USING PARALLEL MULTI-DECISION METHOD

State of protection platen	Number of protection platens	Accuracy	FPR	FNR
on	1,615	99.55%	8.90%	0.45%
off	2,391	96.98%	5.00%	3.02%
standby	1,338	95.33%	4.50%	4.67%

Table II lists the state detection results of Type-II protection platens using the parallel multi-decision method. It is observed that there are 5,344 Type-II protection platens, of which 1,615 are in the "on" state, 2,391 are in the "off" state, and 1,338 are in the "standby" state. As shown in Table III, for the automatic state recognition task of Type-II protection platens the recognition accuracy for the state "on" is 99.55%, that for FPR 8.90%, and that for FNR 0.45%. The recognition accuracy for state "off" is 96.98%, that for FPR 5.00%, and that for FNR 3.02%. The recognition accuracy for state "standby" is 95.33%, that for FPR 4.50%, and that for FNR 4.67%. These results show that the recognition accuracy of Type-II protection platens in three states is above 95%.

D. Experimental Results of Type-II Protection Platen without Multi-decision Scheme

In this work, we propose a new parallel multi-decision technique to recognize the states of Type-II protection platens. To evaluate the effectiveness of this new parallel multi-decision method, the classification results using the single-decision method with the W-CD-SF or YOLOv5 network are listed in Table III.

Table III lists the automatic state recognition results of Type-II protection platens using the single-decision method with the W-CD-SF or YOLOv5 network. As shown in Table III, for the state "on," the recognition accuracy using W-CD-SF is 93.12%, that for FPR 7.68%, and that for FNR 6.88%. The recognition accuracy using YOLOv5 is 98.88%, that for FPR 9.46%, and that for FNR 1.12%. For state "off," the recognition accuracy using W-CD-SF is 89.54%, that for FPR 10.85%, and that for FNR 10.46%. The recognition accuracy using YOLOv5 is 91.61%, that for FPR 6.19%, and that for FNR 8.39%. For state "standby," the recognition accuracy using W-CD-SF is 92.85%, that for FPR 12.08%, and that for FNR 7.15%. The recognition accuracy using YOLOv5 is 93.06%, that for FPR 11.06%, and that for FNR 6.94%. It is shown that for three states the recognition performance of each single-decision method is poorer than that of the proposed

parallel multi-decision method (shown in Table II). The results indicate that the parallel multi-decision method improves the recognition accuracies by 0.68%, 5.86%, and 2.44% for "on," "off," and "standby" states of the protection platen, respectively.

E. Comparison Experiments

To evaluate the effectiveness of the method proposed in this work, we compared the performance of Faster-RCNN and single-shot multi-box detector (SSD) networks with YOLOv5 for Type-I and -II protection platen states recognition tasks.

Faster-RCNN is a two-stage network used for object detection tasks, especially for small objects. It has high detection accuracy and has been widely used in industry [30], [31]. The SSD network is a one-stage network that is based on regression and region proposal algorithms. It can directly predict the position and category of bounding boxes [32,33]. The results of these two deep-learning methods and our proposed method with the YOLOv5 network for recognizing protection platen states are shown in Table IV.

Table IV shows the automatic state recognition results for Type-I and -II protection platens. For Type-I protection platens, the recognition accuracy of state "on" using Faster-RCNN is 96.54% and that using SSD is 89.63%, which are both lower than the accuracy using YOLOv5 (98.77%). The recognition accuracy of state "off" using Faster-RCNN is 92.25% and that using SSD is 90.58%, which are both lower than the accuracy using YOLOv5 (99.15%). For Type-II protection platens, the recognition accuracy of state "on" using Faster-RCNN+W-CD-SF is 97.52%, and that using SSD+W-CD-SF is 90.43%, which are both lower than the accuracy using YOLOv5+W-CD-SF (99.55%). The recognition accuracy of state "off" using Faster-RCNN+W-CD-SF is 95.46% and that using SSD+W-CD-SF is 93.65%, which are both lower than the accuracy using YOLOv5+W-CD-SF (96.98%). The recognition accuracy of state "standby" using Faster-RCNN+W-CD-SF is 96.38% and that using SSD+W-CD-SF is 89.75%, which are both lower than the accuracy using YOLOv5+W-CD-SF (95.33%). The comparison of experimental results indicates that the YOLOv5 is more suitable for automatic protection platen state classification in this work.

The experimental data were collected under various shooting environments and conditions, leading to difficulties in accurately discriminating protection platen state. The methods proposed in this work combine the advantages of YOLOv5 and image processing algorithms and perform well in the state recognition task of two protection platen types.

TABLE III. STATE RECOGNITION RESULTS OF TYPE-II PROTECTION PLATENS USING A SINGLE-DECISION METHOD WITH W-CD-SF OR YOLOV5 NETWORK

State of protection platen	Accuracy		FPR		FNR	
	W-CD-SF	YOLOv5	W-CD-SF	YOLOv5	W-CD-SF	YOLOv5
on	93.12%	98.88%	7.68%	9.46%	6.88%	1.12%
off	89.54%	91.61%	10.85%	6.19%	10.46%	8.39%
standby	92.85%	93.06%	12.08%	11.06%	7.15%	6.94%

TABLE IV. COMPARISON OF EXPERIMENTAL RESULTS

State classification accuracy of Type-I protection platen			State classification accuracy of Type-II protection platen			
Network	State of protection platen		Method	State of protection platen		
	On	off		on	off	standby
Faster-RCNN	96.54%	92.25%	Faster-RCNN +W-CD-SF	97.52%	95.46%	96.38%
SSD	89.63%	90.58%	SSD+W-CD-SF	90.43%	93.65%	89.75%
YOLOv5	98.77%	99.15%	YOLOv5 + W-CD-SF	99.55%	96.98%	95.33%

IV. CONCLUSION

An automatic protection platen state detection method was proposed in this work. In most previous research, experiments were conducted for only one type of protection platen; this was not helpful in practical applications since there are different protection platen types in the natural environment. To solve this problem, we proposed a new system that could classify multiple protection platen types and recognize each protection platen state automatically. First, the automatic classification of Type-I and -II protection platens was realized by the proposed HSV color space weighting operators. Second, the YOLOv5 network was used to detect the Type-I protection platen states. The detection accuracy for two states of Type-I protection platen was over 98%. Then, an automatic state detection system for the Type-II protection platen was presented based on the proposed parallel multi-decision method, combining the proposed W-CD-SF method and the YOLOv5 network. The recognition accuracies of the three states of Type-II protection platen ("on", "off" and "standby") exceeded 95%. Experimental results showed that our newly proposed system could classify multiple protection platen types and recognize each platen state automatically. In addition, the proposed system had good robustness and generalization due to the combination of a deep-learning network and image processing techniques. Future work will focus on the practical application of the proposed system and the classification and identification of other types of protection platens.

ACKNOWLEDGMENT

We thank all our participants for their contributions.

REFERENCES

[1] Yuansheng, C. Qiang, X. Xiaofu, Z. Qijie, and Z. Changsheng, "An intelligent verification method for relay protection pressed board," Journal of Chongqing University, vol. 38, no. 06, pp. 91-98, 2015-12-15. 2015.

[2] Y. Yu, C. Fu, C. Baiqing, Z. Meiyong, Z. Yiran, and Y. Chao, "Research on substation protection hard plate detection and state recognition technology based on deep learning," Technology Innovation and Application, vol. 11, no. 24, pp. 25-29, 2021-08-28. 2021.

[3] X. He and Y. Wang, "Intelligent Recognition System of Substation Hard Platen State Based on Machine Learning," International Conference on Power System Technology (POWERCON), IEEE, 2018, pp. 4320-4325.

[4] R. Wu, W. Zhang, H. Chen, and J. Jiao, "Research on State Recognition of Platen Based on Improved K-means Algorithm," 2020 International Conference on Electrical Engineering and Control Technologies (CEECT), IEEE, 2020, pp. 1-7.

[5] G. Jian, Y. Shiyong, S. Zhengyu, Y. Zheng, L. Zhenhan, and Y. Jingyan, "Research on the identification of protection press plate state based on OTSU-Graham improved algorithm," Electrical Measurement and Instrumentation, pp. 1-9, 2021-05-19. 2021.

[6] Y. Jingyan, S. Zhengyu, G. Jian, and L. Zhenhan, "Research on operation state identification method of protection platen based on image fusion," Electrical Measurement & Instrumentation, vol. 58, no. 08, pp. 88-96, 2021-03-08. 2021.

[7] L. Zhenhan, S. Zhengyu, G. Jian, and Y. Jingyan, "Status identification of substation protection plate based on improved sparse representation," ELECTRONIC MEASUREMENT TECHNOLOGY, vol. 44, no. 23, pp. 86-92, 2021-12-30. 2021.

[8] C. Yueqing et al., "Condition Recognition System for Relay Protection Plate Based on Improved Bag of Feature Algorithm," Power Grid Analysis & Study, vol. 49, no. 02, pp. 99-106, 2021-02-20. 2021.

[9] L. Tiecheng, R. Jiangbo, L. Qingquan, Z. Yuhao, W. Zhihua, and H. Yanjiao, "Image Recognition and Model Cluster Matching of Relaying Plate," JOURNAL OF HARBIN UNIVERSITY OF SCIENCE AND TECHNOLOGY, vol. 26, no. 04, pp. 70-77, 2021-08-27. 2021.

[10] F. Wenlong et al., "Protection platen status recognition based on image processing and morphological feature analysis for smart substation," Electric Power Automation Equipment, vol. 39, no. 07, pp. 203-207, 2019-07-12. 2019.

[11] Y. Tuolai, L. Xinhai, L. Haixin, Z. Lingcheng, M. Chenxu, and Y. Yanhe, "State identification method of relay protection pressing plate based on fast r-cnn algorithm," Electrical Technology and Economy, no. 06, pp. 36-39, 2021-12-20. 2021.

[12] S. Baohua, J. Renyue, Y. Chao, L. Zhenxing, and L. Yanzhang, "Enhanced YOLO network for status recognition of a substation protection plate," Power System Protetion and Control, vol. 49, no. 23, pp. 163-170, 2021-12-01. 2021.

[13] C. Xiang, Z. Qingnian, X. Shaoyu, and C. Cuiqiong, "Identification of Platen Switch State Based on Transfer Learning Strategy," JISUAN]I YU XIANDA IHUA, no. 05, pp. 120-126, 2021-05-15. 2021.

[14] Y. Qianwen and Z. Ke, "Press-Plate State Recognition Based on Improved Bilinear Fine Grained Model," Laser & Optoelectronics Progress, vol. 58, no. 20, pp. 146-155, 2021-10-25. 2021.

[15] D. Wang and D. He, "Channel pruned YOLO V5s-based deep learning approach for rapid and accurate apple fruitlet detection before fruit thinning," Biosyst. Eng., vol. 210, pp. 271-281. 2021.

[16] S. W. Kang and U. S. Choi, "ROI Image Encryption using YOLO and Chaotic Systems," INTERNATIONAL JOURNAL OF ADVANCED COMPUTER SCIENCE AND APPLICATIONS, vol. 12, no. 7, pp. 466-474, 2021-01-01. 2021.

[17] C. Dewi, R. Chen, and H. Yu, "Weight analysis for various prohibitory sign detection and recognition using deep learning," Multimed. Tools Appl., vol. 79, no. 43-44, pp. 32897-32915. 2020.

[18] K. He, X. Zhang, S. Ren, and J. Sun, "Spatial Pyramid Pooling in Deep Convolutional Networks for Visual Recognition," IEEE T. Pattern Anal., vol. 37, no. 9, pp. 1904-1916. 2015.

[19] J. Liu and D. Zhang, "Research on Vehicle Object Detection Algorithm Based on Improved YOLOv3 Algorithm," Journal of physics. Conference series, vol. 1575, no. 1, p. 12150, 2020-01-01. 2020.

[20] T. Lin, P. Dollar, R. Girshick, K. He, B. Hariharan, and S. Belongie, "Feature Pyramid Networks for Object Detection," Proceedings of IEEE Conference on Computer Vision and Pattern Recognition, pp. 2117-2125. 2017.

[21] S. Liu, L. Qi, H. Qin, J. Shi, and J. Jia, "Path Aggregation Network for Instance Segmentation," Proceedings of the IEEE Conference on Computer Vision and Pattern Recognition, pp. 8759-8768. 2018.

[22] H. Rezatofighi, N. Tsoi, J. Gwak, A. Sadeghian, I. Reid, and S. Savarese, "Generalized Intersection over Union: A Metric and A Loss for Bounding Box Regression," Proceedings of the IEEE/CVF Conference on Computer Vision and Pattern Recognition, pp. 658-666, 2019-01-01. 2019.

[23] X. L. Huan, H. Zhou, and J. L. Zhong, "LSB based Image Steganography by using the Fast Marching Method," INTERNATIONAL JOURNAL OF ADVANCED COMPUTER SCIENCE AND APPLICATIONS, vol. 10, no. 3, pp. 1-5, 2019-01-01. 2019.

[24] S. Wang, X. Yan, F. Ma, P. Wu, and Y. Liu, "A novel path following approach for autonomous ships based on fast marching method and deep reinforcement learning," Ocean Eng., vol. 257, p. 111495. 2022.

[25] Y. Qi, "Multi-stencils fast marching method for factored eikonal equations with quadratic anisotropy," Appl. Math. Comput., vol. 417, p. 126776. 2022.

[26] V. Sivakumar and N. Janakiraman, "A novel method for segmenting brain tumor using modified watershed algorithm in MRI image with FPGA," Biosystems, vol. 198, p. 104226. 2020.

[27] A. M. Anter and A. E. Hassenian, "CT liver tumor segmentation hybrid approach using neutrosophic sets, fast fuzzy c-means and adaptive watershed algorithm," Artif. Intell. Med., vol. 97, pp. 105-117. 2019.

[28] L. Zhang, L. Zou, C. Wu, J. Jia, and J. Chen, "Method of famous tea sprout identification and segmentation based on improved watershed algorithm," Comput. Electron. Agr., vol. 184, p. 106108. 2021.

[29] W. Cao, Z. Qiao, Z. Gao, S. Lu, and F. Tian, "Use of unmanned aerial vehicle imagery and a hybrid algorithm combining a watershed algorithm and adaptive threshold segmentation to extract wheat lodging," Physics and Chemistry of the Earth, Parts A/B/C, vol. 123, p. 103016. 2021.

[30] S. Ren, K. He, R. Girshick, and J. Sun, "Faster R-CNN: Towards Real-Time Object Detection with Region Proposal Networks," IEEE Trans Pattern Anal Mach Intell, vol. 39, no. 6, pp. 1137-1149, 2017-06-01. 2017.

[31] R. F. Mansour, J. Escorcia-Gutierrez, M. Gamarra, J. A. Villanueva, and N. Leal, "Intelligent video anomaly detection and classification using faster RCNN with deep reinforcement learning model," Image Vision Comput., vol. 112, p. 104229. 2021.

[32] J. Kim, M. Jung, and J. Kim, "Decoupled SSD: Reducing Data Movement on NAND-Based Flash SSD," IEEE Comput. Archit. L., vol. 20, no. 2, pp. 150-153. 2021.

[33] Z. Shen, L. Han, C. Ma, Z. Jia, T. Li, and Z. Shao, "Leveraging the Interplay of RAID and SSD for Lifetime Optimization of Flash-Based SSD RAID," IEEE T. Comput. Aid. D., vol. 40, no. 7, pp. 1395-1408. 2021.